JOURNAL OF PHYSICAL ORGANIC CHEMISTRY
J. Phys. Org. Chem. 2007; **20:** 463–468
Published online 29 April 2007 in Wiley InterScience
(www.interscience.wiley.com) DOI: 10.1002/poc.1179

Computational studies of the cyclization of thiosemicarbazides

Agata Siwek[1] and Piotr Paneth[2]*

[1]Department of Organic Chemistry, Faculty of Pharmacy, Medical University, Staszica 6, 20–081 Lublin, Poland
[2]Institute of Applied Radiation Chemistry, Technical University, Zeromskiego 116, 90–924 Lodz, Poland

Received 15 January 2007; revised 26 February 2007; accepted 26 February 2007

ABSTRACT: While typically cyclodehydration of thiosemicarbazides in acidic media leads to 1,3,4-thiadiazoles, we have recently shown that under reflux conditions in anhydrous acetic acid the cyclization yields an imidazolidine derivative. The mechanism of this reaction has been characterized theoretically. Calculations indicate that this direction, facilitated by the presence of the —CH_2CO_2— moiety in the N4 substituent is favored over the direction leading toward the thiadiazole product. Formation of the C—N bond that closes the five-member ring appears to be concerted with the departure of ethanol molecule, although the proton transfer from the nitrogen atom to oxygen atom is much more advanced in the transition state. Copyright © 2007 John Wiley & Sons, Ltd.

KEYWORDS: 1,3,4-thiadiazole; cyclization; DFT; theoretical calculations

INTRODUCTION

Derivatives of 1,3,4-thiadiazoles are known to exhibit antibacterial,[1] antifungal,[2] and anticonvulsant[3] activities. Therefore, new thiadiazoles have been synthesized in our laboratory for a long time and their potential pharmacological activities have been investigated. Typically, the compounds could be prepared by the intramolecular dehydrative cyclization of 1,4-disubstituted thiosemicarbazides in acidic medium[4] as presented in Scheme 1.

Therefore, it was expected that the same synthetic procedures should be applicable to the synthesis of 5-(4-methyl-1,3,4-thiadiazol-5-yl)-1,2,3-thiadiazole-2-aminoacetic acid. However, we have recently found,[5] that refluxing 4-ethoxycarbonylmethyl-1-(4-methyl-1,2,3-thiadiazol-5-ylcarbonyl)thiosemicarbazide, **1**, (R = 4-methyl-1,3,4-thiadiazol-5-yl, R^1 = ethoxycarbonylmetonylmethyl in Scheme 1) in anhydrous acetic acid yields an unexpected product, 4-methyl-N-(4-oxo-2-thioxoimidazolidin-3-yl)-1,2,3-thiadiazole-5-carboxamide, **2** (Scheme 2). Apparently, the presence of the —CH_2CO_2— moiety in the R^1 substituent renders formation of the imidazolidine ring derivative energetically favorable. Herein, we present theoretical support obtained using hybrid density functional theory (DFT) for this direction of the cyclization.

**Correspondence to:* P. Paneth, Institute of Applied Radiation Chemistry, Technial University, Zeromskiego 116, 90-924 Lodz, Poland.
E-mail: paneth@p.lodz.pl

COMPUTATIONAL METHODS

Initially a conformational search was performed at the molecular mechanics level using MM+ force field implemented in HyperChem.[6] The conformational space included all seven dihedral angles along the main chain of the reactant **1** and allowed to identify the most stable conformers of this molecule. Subsequently, selected structures were refined using B3PW91 functional,[7] a hybrid DFT level that was shown to be appropriate for activation barriers and heats of reactions,[8] with the standard 6-31G(d) basis set[9] as implemented in the Gaussian package.[10] All calculations were carried out using default convergence criteria. For structures that correspond to substrates of different reaction pathways (see Schemes 1–3), relaxed potential energy surface (PES) scans have been carried out by systematic diminishing of the interatomic distance that leads to the ring closure. The points of maximum energy on these PES scans were used as the starting points for the geometry optimization to the corresponding transition states. Vibrational analysis was performed for the optimized structures to confirm that they represent stationary points on the PESs (3n-6 real normal modes of vibration for the reactant and exactly one imaginary frequency for the transition state) and to calculate gas phase Gibbs free energies. Both neutral species and cations were considered. Solvation free energies were evaluated using two implicit solvent models. The first model that uses the Poisson-Boltzmann method is implemented in the Jaguar program.[11] The second model

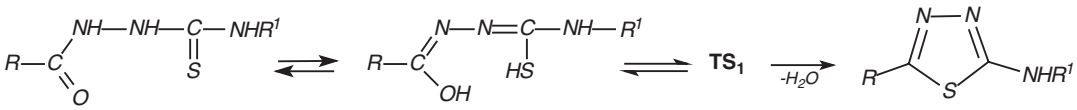

Scheme 1

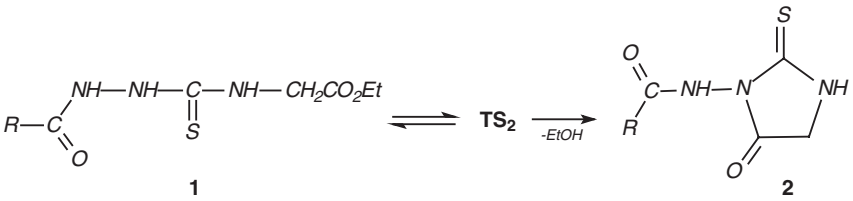

Scheme 2

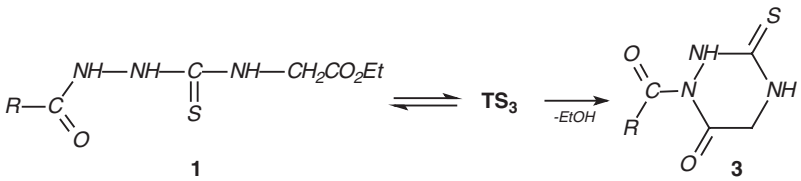

Scheme 3

used, SM5.42,[12] was implemented in the MN-GSM program.[13] The choice of these two models was dictated by the availability of parameters corresponding to acetic acid which was used as the solvent in the experiments.

RESULTS AND DISCUSSION

Conformational search using dihedral angles along the main chain of the reactant **1** allowed us to identify the most stable conformer of this molecule. Its main characteristic feature is a twist around C(5)—N(6)— C(7)—N(9) skeleton (atom numbering is given in Figure 1), which results in placing atoms N(9) and C(3) opposite each other at the distance of about 3 Å. Thus, the most stable conformer is preoriented to ring closure according to Scheme 2. We label this conformation $\mathbf{1}_2$ (reactant **1** in the geometry corresponding to the reaction described by Scheme 2). This structure was

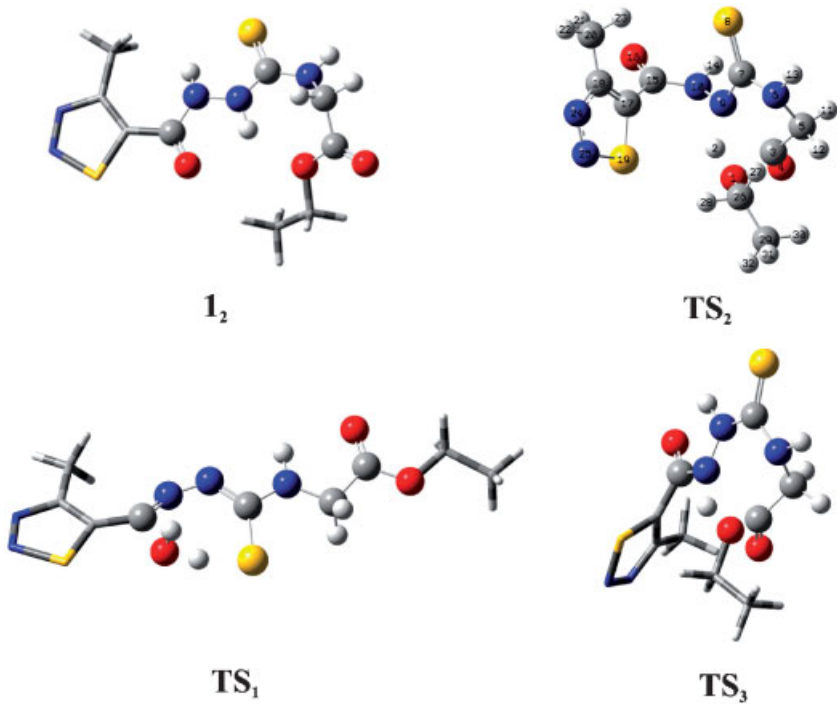

Figure 1. Atom numbering and DFT-optimized structures of the most stable substrate and transition states of reactions illustrated in Schemes 1–3. The substituent R (4-methyl-1,2,3-thiadiazol-5-yl) and ethyl group of R^1 (ethoxycarbonylmethyl) rendered as tubes for clarity

DOI: 10.1002/poc

refined at the DFT level. A relaxed PES scan originated in this structure, with systematic shortening of the N(9)—C(3) distance and subsequent geometry optimization of the point characterized by the energy maximum to the nearest saddle point yielded the structure **TS$_2$** that is the transition state of the reaction given in Scheme 2. It is characterized by one imaginary frequency of 585.7 cm^{-1} that corresponds to the simultaneous formation of N(9)—C(3) and H(2)—O(1) bonds and rupture of the C(3)—O(1) bond. Gibbs free energy of activation corresponding to this transition state is equal to 51.9 kcal/mol at 392 K. Structures of **1$_2$** and **TS$_2$**. are illustrated in Figure 1.

In order to address the influence of the solvent, the structure of **1$_2$** was reoptimized using two different implicit solvent models of acetic acid, SM5.42 and Poisson-Boltzmann. Geometric parameters that undergo major changes on going from the reactant to the transition state, obtained in the gas phase and within the implicit solvent models indicate negligible solvent influence. The same comparison for the transition state **TS$_2$** failed because we were unable to converge the optimization calculations to the transition state when using the SM5.42 model. However, Gibbs free energy of activation calculated from the structures optimized using the Poisson–Boltzmann model, and from the gas phase geometries with energy corrections made with the SM5.42 model differ only by 0.1 kcal/mol. This supports the conclusion that geometric changes caused by solvation are negligible. Therefore, we carried out the rest of our calculations using geometries obtained in the gas phase, with the energy corrections for solvation obtained from the SM5.42 single point calculations, that is, all results reported herein were obtained at the SM5.42/B3PW91/6-31G(d)//B3PW91/6-31G(d) level of theory.

The transition state that leads to the cyclization according to the path illustrated by Scheme 1 (**TS$_1$**) has been optimized. Its electronic energy is 5.7 kcal/mol lower than **TS$_2$**. While exploring PES another reaction channel leading to the product containing a six-member ring that is formed when the cyclization proceeds with ring closure via N(6) and C(12) atoms has been identified. The barrier height of this pathway, presented in Scheme 3, is even lower; the electronic energy of the transition state **TS$_3$** is 1.6 kcal/mol lower than that of **TS$_1$**. Basic geometric and energetic features of the most stable conformer of the reactant **1** and the three transition state structures are collected in Table 1.

It is interesting to note that although electronic energies of the **TS$_1$** and **TS$_3$** structures are lower than that of **TS$_2$**, the Gibbs free energy of activation associated with this latter transition state is the lowest when the zero-point-energy, solvation effects, and thermal contributions at 118.5°C are included.

The comparison of energies of the transition states for the alternative reaction pathways are in agreement with the experimentally observed direction of the cyclization of the reactant. However, only transition states for the concerted pathways have been identified. We have, however, disproved experimentally an alternative, stepwise mechanism with the hydrolysis of the ester and subsequent dehydrocyclization of the corresponding acid.

Table 1. Main geometric parameters, imaginary frequencies, and relative energies of the most stable conformer of the reactant (**1$_2$**) and transition states for reactions given in Scheme (1) (**TS$_1$**), Scheme (2) (**TS$_2$**), Scheme (3) (**TS$_3$**)

Coordinate[a]/property				**1$_2$**	**TS$_1$**	**TS$_2$**	**TS$_3$**
C(3)	O(1)			1.342	1.334	1.647	1.659
C(15)	O(16)			1.233	1.738	1.218	1.231
O(1)	H(2)			2.089	—	1.068	1.379
O(1)	H(14)			—	—	—	1.024
O(16)	H(14)			—	0.975	—	—
N(9)	H(2)			1.022	—	1.502	—
N(10)	H(14)			—	—	—	1.712
S(8)	H(2)			—	1.789	—	—
N(9)	C(3)			3.404	—	2.117	—
N(10)	C(3)			—	—	—	2.156
S(8)	N(15)			—	3.408	—	—
N(9)	H(2)	O(1)		136.0	—	135.0	—
N(10)	H(14)	O(1)		—	—	—	129.3
O(16)	H(2)	S(8)		—	168.6	—	—
N(6)	C(7)	N(9)	N(10)	−179.4	−178.2	−162.0	20.2
C(5)	N(6)	C(7)	N(9)	−18.1	−175.7	37.2	43.7
N(9)	N(10)	C(15)	O(16)	5.2	−6.8	164.8	2.9
N(10)	C(15)	C(17)	S(19)	174.3	172.6	−61.2	55.5
$i\nu^{\neq}$				—	406.4	585.7	278.4
$\Delta E^{\neq}$				—	55.5	61.2	53.9
$\Delta G^{\neq}_{392}$				—	50.3	51.9	53.3
ΔG_{solv}				—	5.3	−4.6	−5.2
$\Delta G^{\neq}_{392} + \Delta G_{solv}$				—	55.6	47.3	48.1

[a] Atom numbering according to Fig. 1, distances in Å, valence and dihedral angles in degrees, imaginary frequencies in cm^{-1} and energies in kcal/mol.

DOI: 10.1002/poc

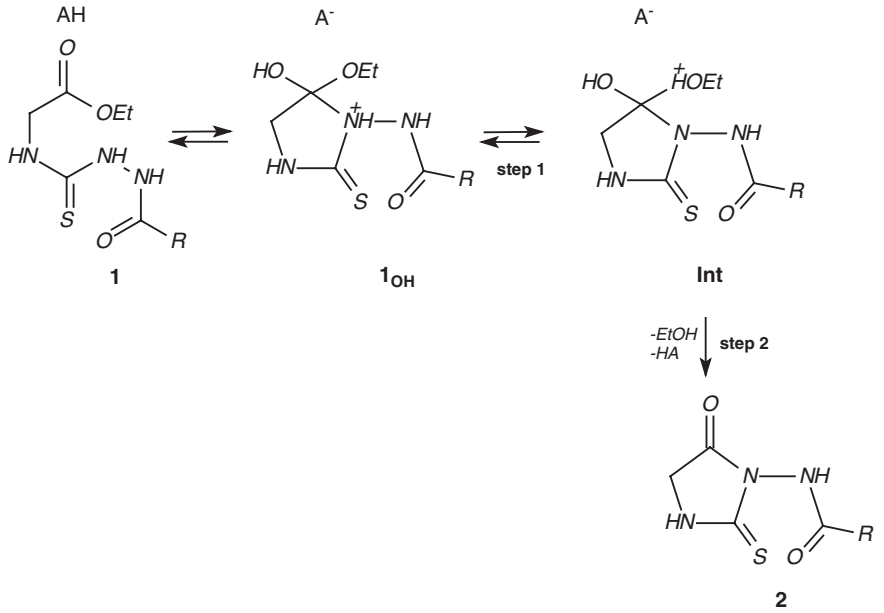

Scheme 4

Reflux of ethyl 3,4-dimethoxyphenylacetate or ethyl phenylacetate, which contains all main features of the substrate of the studied reaction but cannot undergo the cyclization, showed no detectable hydrolysis to the corresponding acids under the same experimental conditions.[14–16]

Two other aspects of the reaction conditions have to be taken into account before drawing conclusions regarding the actual mechanism of the studied reaction. Since it is carried out in anhydrous acetic acid one might expect that the reaction is acid-catalyzed. Furthermore, under such conditions the acid-catalyzed reaction may proceed via a step-wise rather than concerted mechanism. These problems were addressed computationally by considering reactivity of the protonated species.

Calculations carried out for **1** protonated at all possible sites (oxygen, sulphur, and nitrogen atoms) showed that the most stable cation is the one protonated at the nitrogen N(24) of the substituent ring. Optimization of the corresponding protonated transition state yielded Gibbs free energy of activation for the reaction given by Scheme 2 equal to 51.9 kcal/mol, which is 4.6 kcal/mol higher than the corresponding activation barrier for the unprotonated reactants.

As mentioned above, dehydrocyclization reactions carried out in acetic acid may proceed via a stepwise mechanism with acid catalysis as shown in Scheme 4. In fact, this pathway turned out to be energetically preferred over the concerted mechanism in case of substituted phthalanilic acids.[17] We have optimized all stationary

Table 2. Main geometric parameters, imaginary frequencies, and relative energies of the stationary points corresponding to the step-wise mechanism presented in Scheme 4

Coordinate[a]/property				$\mathbf{1_{OH}}$	$\mathbf{TS_{step1}}$	**Int**	$\mathbf{TS_{step2}}$
C(3)	O(1)			1.267	1.280	1.356	1.450
C(15)	O(16)			1.239	1.208	1.207	1.206
O(1)	H(2)			2.354	3.371	2.245	1.220
N(9)	H(2)			1.023	1.021	1.032	1.376
N(9)	C(3)			3.306	2.219	1.594	1.477
N(9)	H(2)	O(1)		131.4	55.4	77.7	110.2
N(6)	C(7)	N(9)	N(10)	−174.9	−73.5	−99.7	133.7
C(5)	N(6)	C(7)	N(9)	−26.3	−9.8	−4.3	11.4
N(9)	N(10)	C(15)	O(16)	6.6	142.1	146.0	147.4
N(10)	C(15)	C(17)	S(19)	175.3	−28.4	−34.3	−55.5
$i\nu^{\neq}$				—	85.2	—	1556.7
$\Delta E^{\neq}$				—	37.3	35.2	62.3
$\Delta G^{\neq}_{392}$				—	37.1	35.2	59.8
ΔG_{solv}				—	−2.9	−3.4	−6.5
$\Delta G^{\neq}_{392} + \Delta G_{solv}$				—	34.2	31.8	53.3

[a] Atom numbering according to Fig. 1, distances in Å, valence and dihedral angles in degrees, imaginary frequencies in cm^{-1} and energies in kcal/mol.

DOI: 10.1002/poc

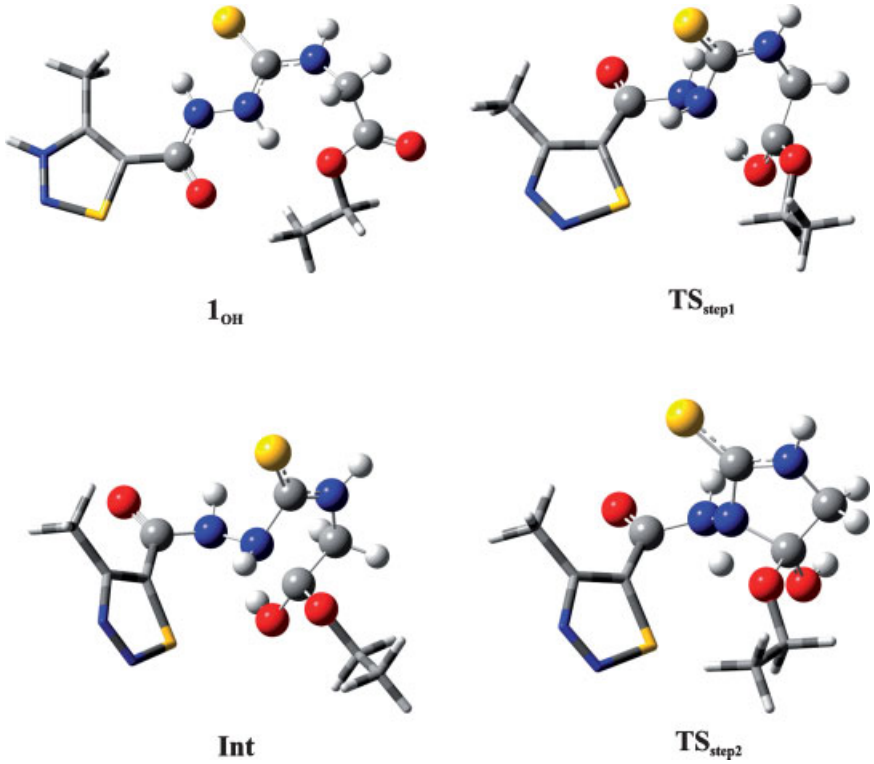

Figure 2. DFT-optimized structures of the stationary points corresponding to the pathway illustrated in Scheme 4. The substituent R (4-methyl-1,2,3-thiadiazol-5-yl) and ethyl group of R^1 (ethoxycarbonylmethyl) rendered as tubes for clarity

points of the mechanism corresponding to Scheme 4. The results of these calculations are summerized in Table 2 and illustrated in Figure 2.

Energetic profile that emerges from the data collected in Table 2 for the step-wise mechanism with acid catalysis comprises formation of the protonated intermediate **Int** that can easily decompose back to the protonated reactant. Gibbs free energy of activation of this reverse step is only 2.4 kcal/mol. Forward decomposition of this intermediate to the product, on the other hand, is characterized by the Gibbs free energy of activation of 20.5 kcal/mol making the overall process 6 kcal/mol less favorable than the concerted mechanism involving neutral species.

In summary, calculations presented herein pinpoint the origins of 4–ethoxycarbonylmethyl-1-(4-methyl-1,2,3-thiadiazol-5-ylcarbonyl)-thiosemicarbazide conversion to 4-methyl-N-(4-oxo-2-thioxoimidazolidin-3-yl)-1,2,3-thiadiazole-5-carboxamide to the most favorable conformation of the reactant that places in the proximity nitrogen and carbon atoms, which are closing the ring. The obtained results advocate for the concerted mechanism of the unprotonated species proceeding through the transition state in which proton transfer to the leaving ethoxy group is slightly more advanced than ring closure and carbon—oxygen bond breaking. While the proton catalysis is not a factor for the studied reaction it should be noted that the presence of the solvent substantially lowers the barrier, which in the gas phase is over 12 kcal/mol higher.

Acknowledgements

We thank Michal Rostkowski for help with SM5.42 calculations. PP acknowledges CNRS support. Access to supercomputing facilities at PCSS Poznan, and Cyfronet, Krakow, Poland and MSI, Minneapolis, MN, USA is acknowledged.

REFERENCES

1. (a) Sherman WR. *J. Org. Chem.* 1961; **26**: 88; (b) Patel HV, Fernandes PS. *J. Indian Chem. Soc.* 1990; **67**: 401; (c) Tsotinis A, Varvaresou A, Calogeropoulou T, Siatra-Papastaikoudi T, Tiligada A. *Arzneim.-Forsch./Drug Res.* 1997; **47**: 307.
2. (a) Mamolo MG, Vio L, Banfi E. *Il Farmaco* 1996; **51**: 71; (b) Dogan HN, Rollas S, Erdeniz H. *Il Farmaco* 1998; **53**: 462; (c) Reddy KR, Mogilaiah K, Swamy B, Sreenivasulu B. *Acta Chim. Hung.* 1990; **127**: 45.
3. Dogan HN, Duran A, Rollas S, Sener G, Uysal MK, Gülen D. *Bioorg. Med. Chem.* 2002; **10**: 2893.
4. (a) Zamani K, Faghihi K, Sangi MR, Zolgharnein J. *Turk. J. Chem.* 2003; **27**: 119;; (b) Misra U, Hitkari A, Saxena AK, Gurtu S, Shanker K. *Eur. J. Med. Chem.* 1996; **31**: 629; (c) Dobosz M, Pachuta-Stec A. *Acta Polon. Pharm.* 1996; **53**: 123.
5. Gorczyca-Wawrzycka I, Siwek A, Dobosz M. *Acta. Cryst. E* 2006; **62**: o864.
6. Hyperchem 7.0, Hypercube, FL, USA, 2002.
7. (a) Becke AD. *Phys. Rev. A* 1988; **38**: 3098; *J. Chem. Phys.* 1993; **98**: 5648; (b) Perdew JP, Chevary JA, Vosko SH, Jackson KA, Pederson MR, Singh DJ, Fiolhais C. *Phys. Rev. B* 1992; **46**: 13584.
8. (a) Lynch BJ, Truhlar DG. *J. Phys. Chem. A.* 2003; **107**: 3898; (b) Zhao Y, Pu J, Lynch BJ, Truhlar DG. *Phys. Chem. Chem. Phys.* 2004; **6**: 673.

DOI: 10.1002/poc

9. (a) Hariharan PC, Pople JA. *Theor. Chim. Acta* 1973; **28**: 213; (b) Francl MM, Pietro WJ, Hehre WJ, Binkley JS, Gordon MS, DeFrees DJ, Pople JA. *J. Chem. Phys.* 1982; **77**: 3654.
10. Frisch MJ, Trucks GW, Schlegel HB, Scuseria GE, Robb MA, Cheeseman JR, Montgomery JA Jr, Vreven T, Kudin KN, Burant JC, Millam JM, Iyengar SS, Tomasi J, Barone V, Mennucci B, Cossi M, Scalmani G, Rega N, Petersson GA, Nakatsuji H, Hada M, Ehara M, Toyota K, Fukuda R, Hasegawa J, Ishida M, Nakajima T, Honda Y, Kitao O, Nakai H, Klene M, Li X, Knox JE, Hratchian HP, Cross JB, Bakken V, Adamo C, Jaramillo J, Gomperts R, Stratmann RE, Yazyev O, Austin AJ, Cammi R, Pomelli C, Ochterski JW, Ayala PY, Morokuma K, Voth GA, Salvador P, Dannenberg JJ, Zakrzewski VG, Dapprich S, Daniels AD, Strain MC, Farkas O, Malick DK, Rabuck AD, Raghavachari K, Foresman JB, Ortiz JV, Cui Q, Baboul AG, Clifford S, Cioslowski J, Stefanov BB, Liu G, Liashenko A, Piskorz P, Komaromi I, Martin RL, Fox DJ, Keith T, Al-Laham MA, Peng CY, Nanayakkara A, Challacombe M, Gill PMW, Johnson B, Chen W, Wong MW, Gonzalez C, Pople JA. *Gaussian 03* Revision D.01 Gaussian Inc, Wallingford CT, 2004.
11. Jaguar version 6.0 Schrodinger LLC New York NY, 2005.
12. Li J, Zhu T, Cramer CJ, Truhlar DG. *J. Phys. Chem. A* 2000; **104**: 2178.
13. Chamberlin AC, Kelly CP, Thompson JD, Xidos JD, Li J, Hawkins PD, Winget GD, Zhu T, Rinaldi D, Liotard DA, Cramer CJ, Truhlar DG, Frisch MJ. *MN-GSM* version 6.0 University of Minnesota Minneapolis MN 55455-0431, 2006.
14. Johnson TB, Rentrew HW. *J. Am. Chem. Soc.* 1925; **47**: 242.
15. Dobosz M, Pachuta-Stec A. *Acta Polon. Pharm.* 1995; **52**: 103.
16. Dobosz M, Pitucha M, Dybala I, Kozioł AE. *Collect. Czech. Chem. Commun.* 2003; **68**: 792.
17. Perry CJ, Parveen Z. *J. Chem. Soc., Perkin Trans.* 2001; **2**: 512.

DOI: 10.1002/poc